

X-ray anomalous scattering and specular reflection in M_V photoabsorption regions

J. M. André, R. Barchewitz, A. Maquet, and R. Marmoret

*Laboratoire de Chimie Physique (Laboratoire Associé au Centre National de la Recherche Scientifique),
Université Pierre et Marie Curie, 11 Rue Pierre et Marie Curie, F-75231 Paris Cedex 05, France*

(Received 14 March 1983)

In this paper we present a detailed investigation of the effects of the anomalous variations of the optical constants on the x-ray specular reflectivity of mirrors, in the vicinity of a characteristic frequency. To this end we have compared the transmission spectra of La, Au, and Th in the M_V photoabsorption region with the reflection spectra obtained in the same spectral ranges. The reflection spectra under grazing incidence have been obtained from either a glass mirror (La) or coated mirrors (Au and ThF_4). A simple theoretical model enables us to account for, at least in a general fashion, the experimental reflectivity.

I. INTRODUCTION

In recent years the availability of intense continuous radiation sources, such as electron synchrotrons and laser-induced hot plasmas, has given rise to a renewed interest in x-ray and x-ray-uv reflectivity determinations. These studies were primarily oriented towards the practical implementation and design of optical systems, such as focusing elements, mirrors, etc. associated with these sources. Within this context it remains essential to determine the efficiency and characteristics of various mirrors under grazing incidence.¹ In addition to these obvious practical applications, it soon became apparent that specular reflectivity measurements may compare favorably with other techniques for determining the optical properties of a material in the x-ray and x-ray-uv range.²⁻⁴

The x-ray reflectivity of a mirror depends on several parameters which, broadly speaking, may be classified into two categories related, respectively, to the surface and bulk properties of the material. For the first category one can mention the roughness and the inhomogeneity of the surface. The knowledge of these parameters and of their influence are of particular importance in relation to the engineering of reflecting optics and accordingly numerous studies⁵⁻⁷ have been motivated.

The other aspect we shall consider here concerns the index of refraction or more precisely the optical constants of the material. As a matter of fact, the reflectivity of a mirror may be directly related to the optical constants, which in turn depend ultimately, through the atomic scattering factors, on the electronic distribution in the material. Obviously, when referring to the "bulk properties" one should keep in mind that in x-ray reflection measurements, and especially under grazing incidence, one in fact probes the surface layers of the mirror.

Most determinations of the optical constants are based on the dispersion (Kramers-Kronig) relations. This approach relies on the evaluation, either theoretical or empirical, of the photoelectric attenuation cross section over a wide range of frequency. Unfortunately, it often appears that both theoretical and experimental determinations of realistic x-ray absorption cross sections meet with

considerable practical difficulties. Note also that from a more fundamental point of view some limitations inherent to the method have been pointed out.⁸ Recently, however, various technical improvements have permitted investigation by more direct experimental determinations based on energy dispersive diffractometry from crystalline samples,⁹ and interferometry.¹⁰ This latter technique has attained a level of accuracy which should permit systematic comparisons with the theoretical data.¹¹

In a previous paper,⁴ hereafter referred to as I, we have presented an alternative method based on the measurement of the specular reflectivity of samples with a high degree of surface smoothness. By determining the reflectivity spectra at several glancing angles, one can deduce via a standard iterative procedure the optical constants at any frequency. The method was applied in an anomalous region (SiK absorption edge in quartz) where typical variations of the optical constants are observed. Such studies in anomalous regions are of considerable interest since they provide valuable information on the inner-shell spectra and the distribution of the unoccupied electronic states in the material.

In this paper we shall adopt a somewhat complementary point of view, showing how the anomalous variations of the optical constants affect the specular reflection spectrum. We have found that the effects of such variations can be particularly well exemplified by considering the case of $3d$ thresholds in various elements. So, for the sake of illustration, we have chosen to study the spectral ranges corresponding to, respectively, the following:

(i) The $3d_{5/2} \rightarrow 4f$ transition in lanthanum which gives rise to an almost perfectly Lorentzian absorption line.¹²⁻¹⁴

(ii) The $3d_{5/2} \rightarrow (6p, 5f + 6d, 5f)$ transitions in gold whose absorption spectrum presents an edge structure which exhibits a typical \tan^{-1} shape.¹⁵

(iii) The $3d_{5/2} \rightarrow 5f$ and $3d_{5/2} \rightarrow 7_{sp}$ transitions in thorium which induce an absorption structure which may be analyzed as a combination of the two preceding cases, i.e., a quasi-Lorentzian absorption line superposed onto a \tan^{-1} edge.¹⁶

In Sec. II we outline the main features of specular re-

flectivity in an anomalous domain, when the absorption cannot be neglected. We discuss in particular the respective influence of the absorption and the dispersion on the reflectivity. As the optical constants may be ultimately deduced from the electronic scattering factors, we present in Sec. III a simple and reliable semiphenomenological approach allowing the evaluation of these latter in the anomalous region, i.e., close to a characteristic absorption frequency. Note that this approach based on a one-electron model cannot account for the solid-state or surface effects, at least in a consistent manner. It provides nevertheless a good basis for discussing the connection existing between the macroscopic reflectivity and the atomic properties of a given material.

Section IV is devoted to a presentation of several typical reflection spectra in M_V absorption regions corresponding to the above mentioned transitions. The experimental results are interpreted with the help of the theoretical method presented in Sec. III. We conclude in Sec. V.

II. X-RAY SPECULAR REFLECTION IN AN ANOMALOUS REGION

For a partially polarized radiation the reflectivity R reads

$$R = \frac{1}{2} [|r_{||}|^2(1+P) + |r_{\perp}|^2(1-P)], \quad (1)$$

where the subscripts $||$ and \perp denote, respectively, the components parallel and perpendicular to the incidence plane, $r_{||}$ and r_{\perp} are the corresponding Fresnel reflection coefficients, and

$$P = (I_{||} - I_{\perp}) / (I_{||} + I_{\perp}), \quad (2)$$

where $I_{||}$ and I_{\perp} are the intensities of each component, and P is the degree of polarization of the radiation.

When absorption can occur, the Fresnel coefficients become complex. They can be expressed in terms of the glancing angle u and the complex dielectric constant $\hat{\epsilon} = \epsilon' + i\epsilon''$, as follows:

$$r_{||} = \frac{\hat{\epsilon} \sin u - (\hat{\epsilon} - \cos^2 u)^{1/2}}{\hat{\epsilon} \sin u + (\hat{\epsilon} - \cos^2 u)^{1/2}}, \quad (3a)$$

$$r_{\perp} = \frac{\sin u - (\hat{\epsilon} - \cos^2 u)^{1/2}}{\sin u + (\hat{\epsilon} - \cos^2 u)^{1/2}}. \quad (3b)$$

The dielectric constant $\hat{\epsilon}$ is then connected with the complex Drude refractive index $\hat{n}_D = n_D + i\beta$, via the relation $\hat{\epsilon} = \hat{n}_D^2$.

In the x-ray range the real part n_D of the Drude index is close to and almost generally less than unity and is accordingly written as $n_D = 1 - \delta$, where typical values of the decrement δ are 10^{-6} – 10^{-5} in the energy range around 10 keV. Note also that the extinction coefficient β is directly connected to the linear photoabsorption coefficient μ of the material through the optical theorem: $\beta = \mu\lambda/4\pi$, where λ is the wavelength of the incident radi-

ation. In the same energy range typical values of β are of the same order of magnitude as δ .

A correct calculation of the reflectivity should take into account the heterogeneity of the waves into the material.¹⁷ Accordingly it is convenient to introduce a complex optical index $\hat{n} = n + ix$ and a heterogeneity parameter \underline{a} defined as $\underline{a} = n \cos \theta$, where θ is the so-called heterogeneity angle formed by the equiphase and the equiamplitude planes. These quantities are related to the dielectric constant via the following expression:

$$2n^2 = [(\epsilon' - \cos^2 u)^2 + (\epsilon'')^2]^{1/2} + \cos^2 u + \epsilon', \quad (4a)$$

$$2x^2 = [(\epsilon' - \cos^2 u)^2 + (\epsilon'')^2]^{1/2} + \cos^2 u - \epsilon', \quad (4b)$$

$$2\underline{a}^2 = [(\epsilon' - \cos^2 u)^2 + (\epsilon'')^2]^{1/2} - \cos^2 u + \epsilon'. \quad (4c)$$

It should be noted that the real and imaginary parts of the index of refraction \hat{n} are not the optical constants as they are usually defined: Indeed, they depend on the glancing angle u . Within this framework the Fresnel coefficients become

$$r_{\perp} = \frac{\sin u - \underline{a} + ix}{\sin u + \underline{a} - ix}, \quad (5a)$$

$$r_{||} = \frac{[(\underline{a} + ix)^2 - \cos^2 u] \sin u - \underline{a} - ix}{[(\underline{a} + ix)^2 - \cos^2 u] \sin u + \underline{a} + ix}, \quad (5b)$$

and the ratio $\rho = |r_{||}|^2 / |r_{\perp}|^2$ is

$$\rho = \frac{(\underline{a} - \cos u \cot u)^2 + x^2}{(\underline{a} + \cos u \cot u)^2 + x^2}. \quad (6)$$

Nevertheless, in conditions relevant to our experiment, i.e., at small glancing angles and in the soft x-ray range, the ratio ρ remains close to unity and the expressions (5a) and (5b) can be shown to become approximately equal:

$$|r_{||}|^2 \simeq |r_{\perp}|^2 \simeq \frac{(u - \underline{a})^2 + x^2}{(u + \underline{a})^2 + x^2}. \quad (7)$$

In this context it is convenient to introduce the dimensionless parameters X and Y , which are related to the glancing angle u and the real and imaginary parts of the Drude index via the simple relations

$$X = \frac{u}{\sqrt{2}|\delta|}, \quad Y = \frac{\beta}{\delta}. \quad (8)$$

Then, the parameters \underline{a} and x may be written

$$\underline{a} = \frac{1}{\sqrt{2}} [(T^2 + Y^2)^{1/2} + T]^{1/2} \frac{u}{X}, \quad (9a)$$

$$x = \frac{1}{\sqrt{2}} [(T^2 + Y^2)^{1/2} - T]^{1/2} \frac{u}{X}, \quad (9b)$$

where $T = X^2 - 1$ if $n_D < 1$ and $T = X^2 + 1$ if $n_D > 1$. The final approximate expression of R , we shall use hereafter, reads accordingly:

$$R = \frac{\{\sqrt{2}X - [(T^2 + Y^2)^{1/2} + T]^{1/2}\}^2 + [(T^2 + Y^2)^{1/2} - T]}{\{\sqrt{2}X + [(T^2 + Y^2)^{1/2} + T]^{1/2}\}^2 + [(T^2 + Y^2)^{1/2} - T]}. \quad (10)$$

The dependence of R in terms of X and Y is shown in the Fig. 1. The curves $R = R(X)$ display important changes

when Y varies. For smaller values of Y , when absorption is negligible, the curve has a steplike shape, corresponding to total reflection for $X < 1$, i.e., $u < u_c = \sqrt{2\delta}$, u_c being the so-called critical angle. In this domain as Y increases, the step becomes less pronounced until $Y \simeq 0.63$, a value for which the inflexion point disappears. For higher values of Y when absorption is dominant with respect to dispersion, the reflectivity decreases uniformly when X increases. This behavior is better understood by considering the derivatives $(\partial R / \partial X)_Y$ and $(\partial^2 R / \partial X^2)_Y$, whose variations in terms of X are given in Figs. 2(a) and 2(b). As a matter of fact, one has, respectively:

$$\left(\frac{\partial R}{\partial X} \right)_Y = - \frac{8\sqrt{2}(1+Y^2)[(T^2+Y^2)^{1/2}+T]^{1/2}}{(T^2+Y^2)^{1/2}(\{\sqrt{2}X+[(T^2+Y^2)^{1/2}+T]^{1/2}\}^2+(T^2+Y^2)^{1/2}-T)^2}, \quad (11)$$

and

$$\left(\frac{\partial^2 R}{\partial X^2} \right)_Y = \frac{8R}{T^2+Y^2} \left[[(T^2+Y^2)^{1/2}+T] + \frac{X}{\sqrt{2}} \left[\frac{T[(T^2+Y^2)^{1/2}+T]-Y^2}{2(T^2+Y^2)^{1/2}[(T^2+Y^2)^{1/2}+T]^{1/2}} \right] \right]. \quad (12)$$

From these relations one can easily deduce that an inflexion point, corresponding to an extremum of $(\partial R / \partial X)_Y$ and to a zero of $(\partial^2 R / \partial X^2)_Y$, actually occurs if and only if $Y \leq 0.63$. The disappearance of the inflexion point can be considered as indicating the transition between the steplike and the smooth variation of R in terms of the glancing angle u . Note that, when it exists, the position of the inflexion is located at values of X slightly smaller than $X = 1$, ($u = u_c$). It is interesting to note also [see Figs. 1, 3(a), and 3(b)], that, for a fixed value of X , the reflectivity begins to decrease when Y increases, then reaches a minimum at $Y = (3 - 2X^2)^{1/2}$ and increases again with Y , i.e., when the absorption becomes more important. This minimum in the curves $R = R(Y)$ disappears only for higher values of $X \geq \frac{1}{2}\sqrt{6}$, values for which the derivative $(\partial R / \partial Y)_X$ remains positive:

$$\left(\frac{\partial R}{\partial Y} \right)_X = \frac{4\sqrt{2}XY[(T^2+Y^2)^{1/2}+T-1][(T^2+Y^2)^{1/2}+T]^{-1/2}}{(T^2+Y^2)^{1/2}(\{\sqrt{2}X+[(T^2+Y^2)^{1/2}+T]^{1/2}\}^2+(T^2+Y^2)^{1/2}-T)^2}. \quad (13)$$

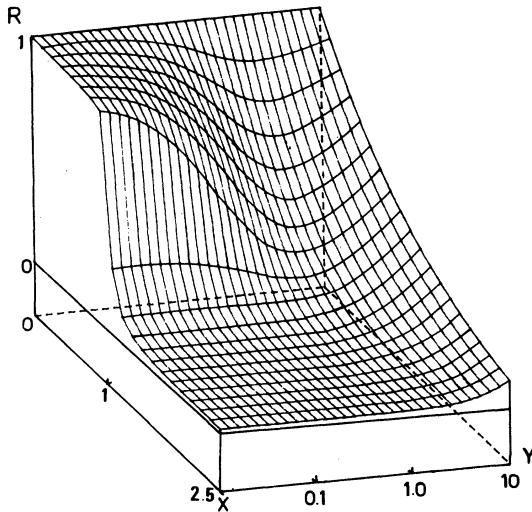


FIG. 1. Variations of the reflectivity R in terms of the dimensionless parameters $X = u/u_c$ and $Y = \beta/\delta$. Here u is the glancing angle, $u_c = \sqrt{2\delta}$ is the so-called critical angle, the decrement $\delta > 0$ is the deviation from unity of the real part of the Drude index \hat{n}_D , and the extinction coefficient β is the imaginary part of \hat{n}_D . One can check in the figure that if the absorption is negligible as compared to the dispersion ($\beta \ll \delta$ or $Y \ll 1$), the reflectivity reveals a steplike variation in terms of the glancing angle u , giving rise to total reflection at small angles ($u < u_c$ or $X < 1$). On the contrary, if absorption increases one observes a smoother variation of R in terms of u , the decrease being less marked as β becomes dominant with respect to δ ($Y > 1$).

In this case ($X \geq \frac{1}{2}\sqrt{6}$) the reflectivity, which is very low when the absorption is negligible ($Y \simeq 0$), increases steadily with Y . Note that these results enable us to give an analytical expression of the weight factor $\varphi = (\partial\beta/\partial\delta)_R$ introduced by Martens and Rabe.¹⁸ This factor provides useful information on the respective contributions of small changes in β and δ on the overall variations of the reflectivity R . After some standard algebra one easily obtains

$$\varphi = \left(\frac{\partial\beta}{\partial\delta} \right)_R = Y - \frac{(1+Y^2)[(T^2+Y^2)^{1/2}+T]}{Y[(T^2+Y^2)^{1/2}+T-1]}. \quad (14)$$

The variations of φ in terms of Y and X are displayed in Fig. 4. These latter are to be compared with Fig. 2 of Ref. 18.

III. COMPUTATION OF THE ANOMALOUS SCATTERING FACTORS

Any theoretical evaluation of the optical constants of a given medium is based on the well-known formula connecting the complex Drude refractive index \hat{n}_D and the forward-scattering amplitude

$$\hat{n}_D = 1 + 2\pi r_0 \left[\frac{c}{\omega} \right]^2 \sum_i N_i F_i(\omega), \quad (15)$$

where ω is the frequency of the incident radiation, r_0 is the classical radius of the electron, N_i stands for the number per unit of volume of scatterers i , with forward-scattering amplitude $F_i(\omega)$. When an absorption process can take place, which is the case we are precisely interested in, $F_i(\omega)$ becomes complex and one can easily establish

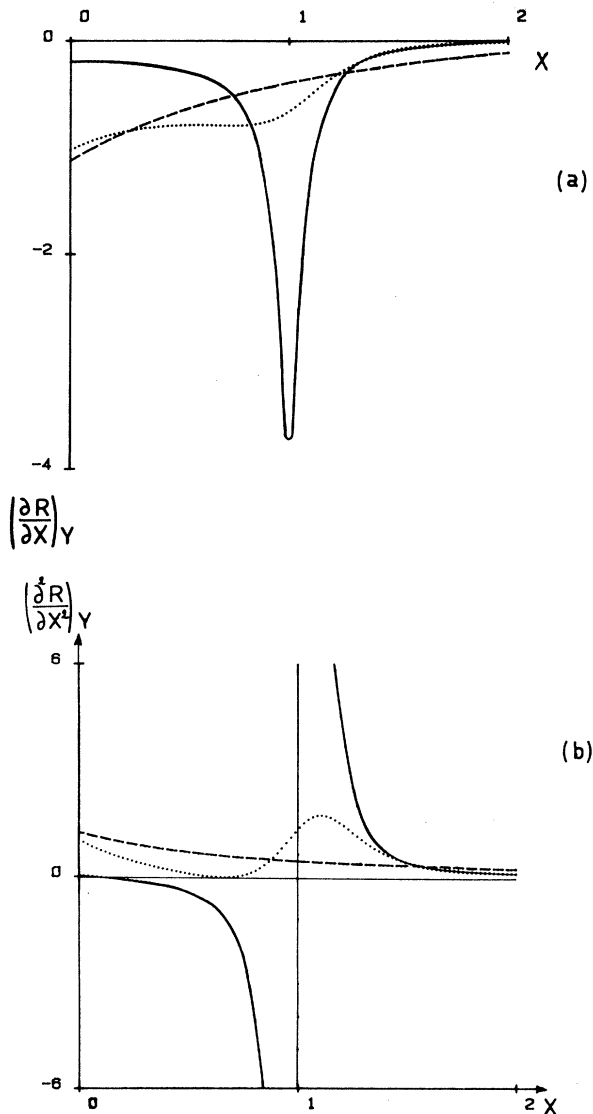


FIG. 2. Variations of the partial derivatives (a) $(\partial R/\partial X)_Y$ and (b) $(\partial^2 R/\partial X^2)_Y$. Solid line, $Y=0.1$; dotted line, $Y=0.63$; dashed line, $Y=5$. The existence of a minimum of $(\partial R/\partial X)_Y$ corresponding to a zero of $(\partial^2 R/\partial X^2)_Y$ indicates the presence of an inflexion point in the curve $R=R(X)$. One observes that the inflexion point disappears if $Y > 0.63$.

the correspondence between the decrement δ and the extinction coefficient β with, respectively, the real and imaginary parts of $F_i(\omega)$.

The main problem encountered when attempting to obtain theoretical estimates of \hat{n}_D is to derive a practical and reliable technique for computing the forward scattering amplitude $F(\omega)$ for an atomic electron. In the case of an unpolarized incident radiation, $F(\omega)$ is given by the modified Kramers-Heisenberg formula:

$$F(\omega) = \frac{\omega^2}{2} \sum_n \frac{g_{n,0}}{\omega_{n,0}} \left[\frac{1}{\omega_{n,0} - \omega - i\Gamma_n/2\hbar} + \frac{1}{\omega_{n,0} + \omega - i\Gamma_n/2\hbar} \right], \quad (16)$$

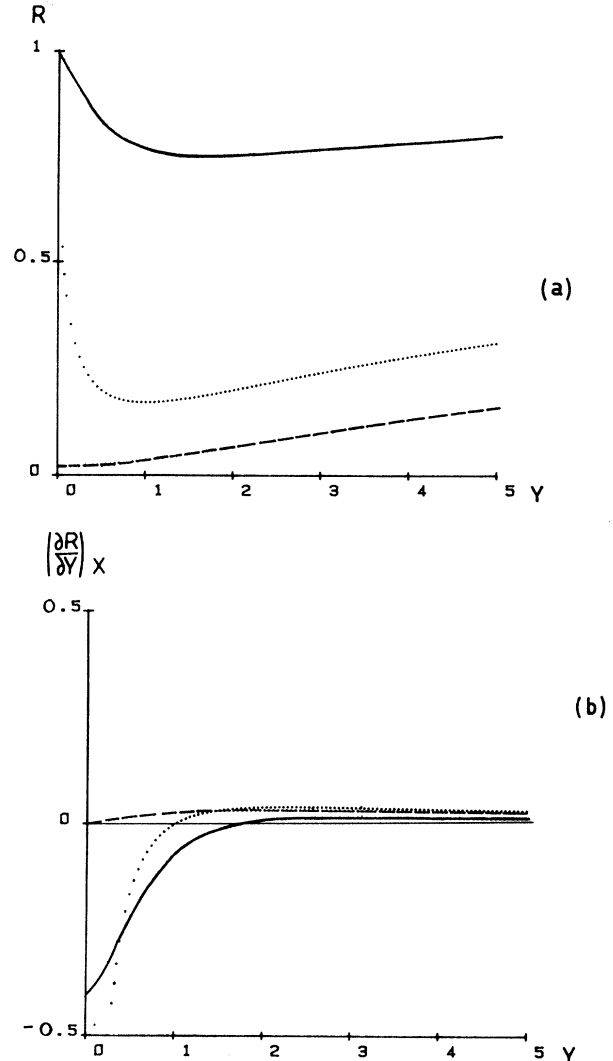


FIG. 3. Variations (a) of the reflectivity R at fixed values of X and (b) of the derivative $(\partial R/\partial Y)_X$ in terms of Y . Solid line, $X=0.2$; dotted line, $X=1$; dashed line, $X=1.5$. The derivative $(\partial R/\partial Y)_X$ can be 0, for finite values of Y only if $X \leq \frac{1}{2}\sqrt{6}$. Otherwise the derivative remains positive, indicating the absence of minimum in the curve $R=R(Y)$.

where the infinite sum runs over the complete set of excited states $|n\rangle$ of energy E_n , $g_{n,0}$ denotes the oscillator strength associated with the transition $|0\rangle \rightarrow |n\rangle$ with characteristic energy $E_{n,0} = \hbar\omega_{n,0} = (E_n - E_0)$. The inclusion of the widths Γ_n of the excited states $|n\rangle$ in the Kramers-Heisenberg formula permits ensuring its validity at resonance, i.e., when $\omega = \omega_{n,0}$.

As already noted in I, if absorption can take place between the initial state and a discrete excited state (or a narrow set of discrete states) the analysis is standard in that case and accordingly will not be reconsidered in this section. By contrast, the case of transitions to a continuum of states is more involved and deserves a closer investigation. As a matter of fact, the summation becomes an integration over the continuous set of excited states distributed according to a density of oscillator strengths $(dg/d\omega)$:

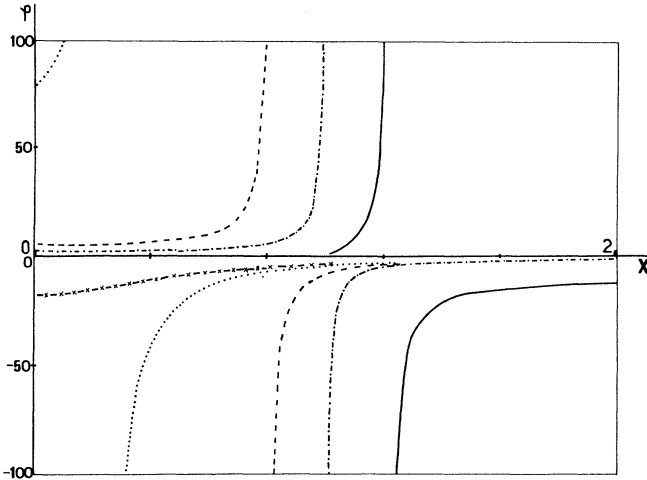


FIG. 4. Variations of the weight factor $\varphi = (\partial\beta/\partial\delta)_R$ in terms of X . Solid line, $Y=0.1$; dotted-dashed line, $Y=1$; dashed line, $Y=1.3$; dotted line, $Y=1.7$; - \times - line, $Y=1.9$. The curves $\varphi = \varphi(X)$ present a discontinuity if $Y < \sqrt{3}$: This indicates that for any given value of Y in this range there exists a value of the glancing angle u in the vicinity of which a small change in δ (respectively β) induces a large change in β (respectively δ).

$$F(\omega) \simeq \frac{\omega^2}{2} \int_0^\infty d\omega' \left[\frac{dg}{d\omega'} \right] \frac{1}{\omega'} \times \left[\frac{1}{\omega' - \omega - i\Gamma(\omega')/2\hbar} + \frac{1}{\omega' + \omega - i\Gamma(\omega')/2\hbar} \right]. \quad (17)$$

In the first approximation, the corresponding widths $\Gamma(\omega')$ can be assumed to be equal to the width Γ of the core hole no matter what the excited states $|n\rangle$ belonging to the continuum: $\Gamma(\omega') \simeq \Gamma$. The latter depends on the various processes contributing to the decay of the excited state, including radiative (fluorescence) and nonradiative ones such as Auger and Coster-Kronig effects. Sensible estimates of Γ may be found in the literature.

The density of oscillator strengths, in the neighborhood of a q edge, is assumed to follow a simple inverse power law in terms of the frequency:

$$\left[\frac{dg}{d\omega} \right]_q = g_q \frac{\alpha - 1}{\omega_q} \left[\frac{\omega_q}{\omega} \right]^\alpha \Theta(\omega - \omega_q), \quad (18)$$

where $\Theta(x)$ stands for the Heaviside step function, ω_q and g_q are, respectively, the edge frequency and the total oscillator strength of the inner shell q , and α is an adjustable parameter, the value of which is usually between $\frac{5}{2}$ and 3. Again relatively accurate values of g_q (Ref. 19) and α , (Ref. 20) are tabulated and can be safely used in such calculations.

When substituting (18) into (17) one can easily obtain, as shown in I, $\text{Re}F(\omega)$ and $\text{Im}F(\omega)$ in terms of Gauss hypergeometric functions ${}_2F_1(a, b; c; z)$, and one has

$$\text{Re}F(\omega) = - \left[\frac{\omega}{\omega_q} \right]^2 g_q \frac{\alpha - 1}{2(\alpha + 1)} \times \left[{}_2F_1 \left[1, \frac{\alpha + 1}{2}; \frac{\alpha + 3}{2}; z^2 \right] + \text{c.c.} \right], \quad (19a)$$

$$\text{Im}F(\omega) = i \left[\frac{\omega}{\omega_q} \right]^2 g_q \frac{\alpha - 1}{2(\alpha + 2)} z^2 \times \left[{}_2F_1 \left[1, \frac{\alpha + 2}{2}; \frac{\alpha + 4}{2}; z^2 \right] - \text{c.c.} \right], \quad (19b)$$

where $z = (\omega + i\Gamma/2\hbar)/\omega_q$. These formulas have been obtained from Eqs. (19a) and (19b) in I by using the relations

$${}_2F_1(1, \alpha + 1; \alpha + 2; z) + {}_2F_1(1, \alpha + 1; \alpha + 2; -z) = 2 {}_2F_1 \left[1, \frac{\alpha + 1}{2}; \frac{\alpha + 3}{2}; z^2 \right], \quad (20a)$$

and

$${}_2F_1(1, \alpha + 1; \alpha + 2; z) - {}_2F_1(1, \alpha + 1; \alpha + 2; -z) = 2z \frac{\alpha + 1}{\alpha + 2} {}_2F_1 \left[1, \frac{\alpha + 2}{2}; \frac{\alpha + 4}{2}; z^2 \right]. \quad (20b)$$

These hypergeometric functions have a series expansion converging in the unit disc $|z^2| < 1$ and can be easily evaluated when the variable verifies this condition. However, since we are interested in the anomalous region $\omega \sim \omega_q$ and since $\Gamma/2\hbar$ is usually very small, $\Gamma/(2\hbar\omega) \ll 1$, one often has $|z^2| \sim 1$, which makes the series converge very slowly or even diverge. It is then convenient to use an analytic continuation process which corresponds to the variable change $z^2 \rightarrow 1 - z^2$.²¹ By specializing the general formula one has

$${}_2F_1(1, b; b + 1; z^2) = -b \ln(1 - z^2) \sum_{n=0}^{\infty} \frac{(b)_n}{n!} (1 - z^2)^n + b \sum_{n=0}^{\infty} \frac{(b)_n}{n!} (1 - z^2)^n \times [\psi(n + 1) - \psi(b + n)], \quad (21)$$

where $(b)_n = \Gamma(b + n)/\Gamma(b)$ and $\psi(z)$ is the logarithmic derivative of the Gamma function. This may be transformed further and after some simple algebra one obtains

$${}_2F_1(1, b; b + 1; z^2) = -b \ln(1 - z^2) z^{-2b} - b(b - 1) \sum_{n=0}^{\infty} \frac{(b)_n}{n!} (1 - z^2)^n \times \sum_{m=n}^{\infty} \frac{1}{(m + 1)(m + b)}. \quad (22)$$

As $1 - z^2$ is relatively small in the vicinity of the critical

frequency, the convergence of the sum is excellent. The remaining problem is to compute accurate values of the coefficients:

$$A_n(b) = \sum_{m=n}^{\infty} \frac{1}{(m+1)(m+b)}. \quad (23a)$$

This can be done by noting that

$$A_n(b) = S(b) - \sum_{p=0}^{n-1} \frac{1}{(p+1)(p+b)} \quad (23b)$$

with

$$S(b) = \sum_{m=0}^{\infty} \frac{1}{(m+1)(m+b)} = (b-1)^{-1} [\psi(b) + \gamma],$$

where $\gamma = 0.577\dots$ is Euler's constant. The series $S(b)$ can be evaluated in various ways to within any desired accuracy, whether b is rational or not.

At higher frequencies, i.e., when $\omega \gg \omega_g$, $z^2 > 1$ and it is convenient to use another analytical continuation formula corresponding to the variable change $z^2 \rightarrow z^{-2}$. One obtains in that case:²¹

$$\begin{aligned} {}_2F_1(1, b; b+1; z^2) &= \frac{-b}{b-1} z^{-2} {}_2F_1(1, 1-b; 2-b; z^{-2}) \\ &\quad + \frac{\pi b}{\sin \pi b} (-z^2)^{-b}, \end{aligned} \quad (24)$$

the convergence rate of the new hypergeometric function becoming excellent. Note that we have extensively used the above formulae in our numerical calculations which were performed on a Commodore Model PET 8032 microcomputer.

IV. COMPARISON OF EXPERIMENT AND THEORY

In this section we shall compare the theoretical predictions obtained from expressions (19a) and (19b) with several experimental reflection spectra obtained in the absorption region for different materials. For the sake of illustration, we have chosen three different cases, associated respectively with three distinct types of photoabsorption transitions. As a matter of fact, the shapes of the dispersion curves in an anomalous region are noticeably different according to whether the corresponding photoabsorption process involves final unoccupied states discrete or not.

As a good illustration of the first case (transition involving discrete final states) we have used a mirror containing a high proportion of lanthanum whose M_V absorption spectrum displays a typical Lorentzian line. The case of a transition towards a broad continuum will be illustrated by the M_V absorption threshold of gold which displays, in first approximation, a typical \tan^{-1} feature. Finally, we shall present a third set of results corresponding to an intermediate situation, illustrated by the region of the M_V absorption of thorium, in which the photoabsorption transition to an unoccupied state distribution comprising both discrete states and a continuum takes place.

It should be noted here that the experimental spectra we

shall present are not normalized to the same reflectivity (or transmitted intensity) scale. In fact, they correspond to different exposure times chosen so as to obtain comparable blackening intensities on the films. Absolute determination of the reflectivity requires much more sophisticated techniques (see in particular Ref. 4) and was beyond the scope of this paper, which is restricted to a qualitative discussion of the general shape of the reflectivity spectra in anomalous regions.

A. La M_V absorption region

The experiment has been carried out with the help of the synchrotron radiation provided by the Anneau de Collisions d'Orsay (ACO) facility. The mirror under study contained 50 wt. % La_2O_3 . The specular reflection spectrum has been analyzed in a continuous range of frequencies, in the vicinity of the M_V absorption of lanthanum ($E = 835.2$ eV), by a vacuum spectrograph.²² The analyzer used here was a mica, 250-mm-radius bent crystal, oriented under a mean Bragg angle $\varphi = 47^\circ$. The detector was a Kodak SA3 film. In order to suppress shorter wavelength radiations, which could be reflected in higher order by the analyzer, we have used a low-pass filter made up of two parallel plane silica SiO_2 mirrors.²³

The M_V photoabsorption spectrum of trivalent lanthanum corresponding to the transition $3d^{10} \rightarrow 3d^9 4f^1$, has been the object of several studies. The spectrum displays an almost perfect Lorentzian line [see Fig. 5(a)], the width at half-height of which being $\Gamma \simeq 1.8$ eV. The linear absorption coefficient, at the maximum of the line, has been determined from a transmission experiment to be $\mu_{\max} \simeq 250\,000 \text{ cm}^{-1}$.²⁴

The spectra of the radiation reflected from the mirror are presented in Fig. 5, at three representative values of the glancing angle u . At small angles u the spectra present a minimum slightly shifted towards the lower energies with respect to the position of the photoabsorption line. When u increases, whereas one observes a global decrease of intensity, a maximum shows up, slightly shifted towards the higher-energy side of the absorption line. The shift of this maximum decreases steadily until $u \simeq 50$ mrad and becomes constant beyond. For instance, at $u \simeq 70$ mrad most of the reflected intensity is localized in a slightly asymmetric line, 2.2 eV wide and shifted 1 eV with respect to the absorption line. Note that the neighborhood of the M_{IV} absorption also induces a light anomaly of the refractive index, which makes the M_V line take shape at smaller angles u than if the M_V absorption line were isolated.

In order to account for the observed spectral distribution of the reflected intensity we have introduced, in the theoretical expressions Eq. (17), the width $\Gamma_{\text{expt}} = 1.8$ eV and the oscillator strength $g_{\text{expt}} = 0.15$ deduced from the previously given value of μ_{\max} . The contribution of the other atomic characteristic transitions has been evaluated with the help of the Cauchois and Sénémaud table,²⁵ and the Cromer table,¹⁹ for the oscillator strengths.

In the anomalous region the decrement presents two extrema situated, respectively, at the energies E_m and E_M corresponding to the half-height of the absorption line; see Fig. 6(a). If the real part of the refractive index is less

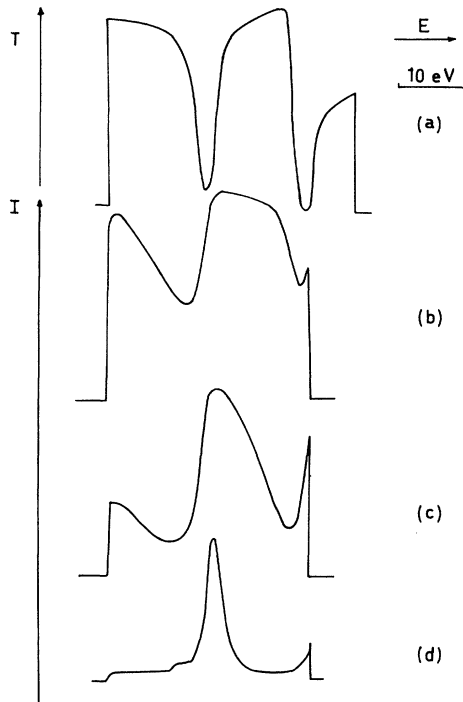


FIG. 5. (a) Transmission spectrum of La_2O_3 in the $M_V(3d^{10} \rightarrow 3d^9 4f^1)$ photoabsorption region of La. (b)–(d) Spectra of the reflected radiation from a glass mirror containing 50 wt. % La_2O_3 in the same spectral range, at different glancing angles u : (b), $u = 20$ mrad; (c), $u = 35$ mrad; (d), $u = 70$ mrad.

than unity (which is precisely the case here) one has $\delta_m < \delta_M$ and consequently $X_m > X_M$, where the indices (m, M) refer, respectively, to the energies of the minimum E_m and of the maximum E_M . One may thus easily check on the curves $R = R(X)$, Fig. 1, that the reflectivities verify the inequality $R_m > R_M$; see Fig. 6. In fact, the actual variations of Y do contribute to reinforce this effect. This explains the occurrence of a maximum of reflectivity M' , which gradually narrows as u increases, revealing eventually the appearance of a “black line” on the experimental spectra.

One notes a slight discrepancy between the experimental and theoretical angular dependence of the general shape of the reflectivity dispersion curves. It is likely that this may be ascribed to both surface roughness and uncertainties affecting the experimental value of the linear absorption coefficient μ_{\max} . This point will be discussed further in Sec. V.

B. Au M_V absorption region

The reflectivity of a gold-coated mirror has been analyzed in the vicinity of the Au M_V absorption edge, which presents a typical \tan^{-1} shape and is located near 2.2 keV. The continuous x-ray source was a classical tube operated at 4.2 keV. Under these conditions the use of a low-pass filter was not necessary, which allowed us to use a simplified version of the experimental setup previously described. The same bent-crystal spectrograph has been used, the analyzer now being a 1010 quartz crystal orient-

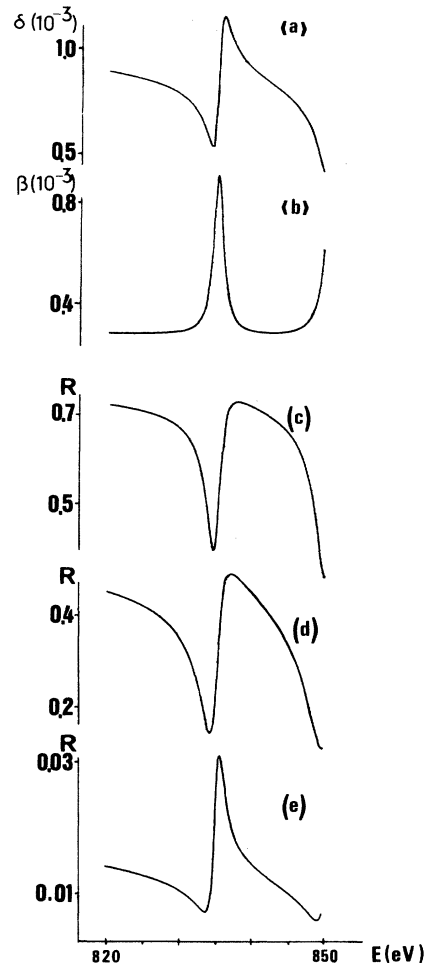


FIG. 6. Variations of the decrement δ of the extinction coefficient β and of the reflected intensity R for a glass mirror containing 50 wt. % La_2O_3 in the M_V photoabsorption region of La, as they are obtained from the theoretical model presented in Sec. III. (a) Variations of δ in terms of the energy; (b) variations of β in terms of the energy; (c)–(e) reflection spectra at different glancing angles: (c), $u = 20$ mrad; (d), $u = 35$ mrad; (e), $u = 70$ mrad.

ed under a mean Bragg angle $\varphi = 40^\circ 30'$. Again, the detector was a Kodak SA3 film.

In Fig. 7(a) we reproduce the transmission spectrum of Au in the M_V -edge region, obtained with the same spectrometer. The spectrum has been obtained by transmission through a few thousand angstrom thick screen, prepared under vacuum by thermal evaporation onto a thin Makrofol film. See also Ref. 15.

The experimental reflection spectra at several representative glancing angles u are presented in Fig. 7. As already noted in similar cases,²⁶ the reflection spectrum mimics the transmission one at small glancing angles $u \lesssim 10$ mrad. When u increases, though the global reflected intensity decreases, the jump gradually becomes a dip. At higher values of $u \gtrsim 15$ mrad the spectral distribution displays a quasisymmetrical feature, the shape of which is similar to the variations of the decrement δ . Then the minimum of reflectivity is located at almost the same en-

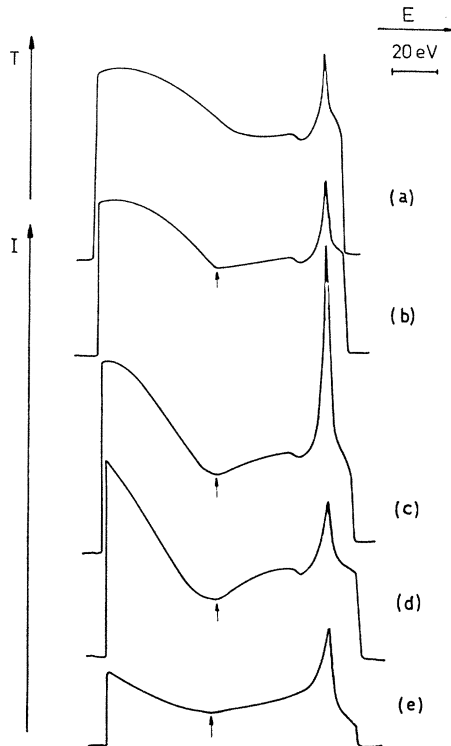


FIG. 7. (a) Transmission spectrum of Au in the M_V -edge-absorption region. The $MoL\alpha$ line (2292 eV) has been used as a reference in energy. (b)–(e) Reflection spectra at different glancing angles: (b), $u=10$ mrad; (c), $u=15$ mrad; (d), $u=17$ mrad; (e), $u=20$ mrad.

ergy than the minimum in the dispersion curve.

Again, the observed reflection spectra can be accounted for with the help of the theoretical model described above in the case of transitions involving final states which belong to a continuum. We used Cromer's values¹⁹ of the oscillator strength associated with the absorption edge. The relevant values of the parameter α and of the photo-absorption coefficient at the bottom of the edge were extracted from the absorption tables of Leroux and Thinh.²⁰ Our theoretical results are presented in the Fig. 8. At small glancing angle $u \lesssim 15$ mrad the general shape of the experimental spectra is very well reproduced by the theory. However, for higher values of u , the theoretical predictions seem to overestimate the magnitude of the reflected intensity.

C. Th M_V absorption region

The reflectivity of a thin film of ThF_4 deposited on a glass mirror has been studied in the Th M_V absorption region, i.e., around 3300 eV. Absorption of the incident radiation can take place to final states belonging either to a continuum or to a narrow localized distribution. The corresponding absorption line is attributed to the transitions $3d^{10} \rightarrow 3d^9 5f^{1,27}$.

The experimental setup is identical to the one used in the preceding experiment on Au, the crystal analyzer now being oriented to a mean Bragg angle $\varphi=49^\circ$. The photo-

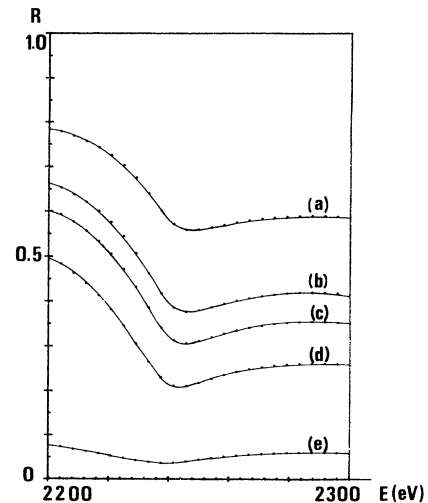


FIG. 8. Reflection spectra for Au in the M_V -edge-absorption region, at different glancing angles u , obtained from the theoretical model presented in the Sec. III. (a), $u=10$ mrad; (b), $u=15$ mrad; (c), $u=17$ mrad; (d), $u=20$ mrad; (e), $u=30$ mrad.

absorption spectrum, observed by transmission through a ThF_4 screen, 5000 Å thick, deposited on a Makrofol sheet, is presented in Fig. 9. The $AgL\beta_{2,15}$ line has been used as a reference on the energy scale. The transmission spectrum presents a pronounced dip m followed by a maximum M .

In Fig. 9 we also display the experimental spectral dis-

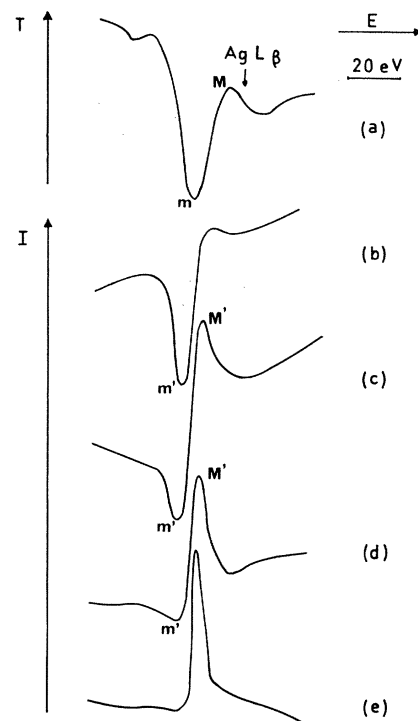


FIG. 9. (a) Transmission spectrum of ThF_4 in the M_V absorption region of Th. The $AgL\beta_{2,15}$ line (3348 eV) has been used as a reference in energy. (b)–(e) Reflection spectra at different glancing angles: (b), $u=7$ mrad; (c), $u=9$ mrad; (d), $u=11$ mrad; (e), $u=13$ mrad.

tribution of the reflected radiation at several glancing angles u between 7 and 13 mrad. Schematically the distribution may be considered as a combination of the limiting cases considered above. At smaller values of u the reflectivity spectrum mimics the transmission one, though the ratio of intensities is globally inverted. In addition, the induced minimum m' is slightly shifted towards lower energies with respect to its homologous m ; see Fig. 9(a).

As u increases, a maximum of intensity M' is evident, which gradually dominates the structure m' . Note that the structure of the feature M' is asymmetric, the rise of intensity being steeper on the low-energy side. Note also that M' is slightly shifted towards higher energies with respect to the maximum of absorption but becomes closer as u increases.

Again this behavior can be accounted for, at least in a general fashion, by using the theoretical analysis of Sec. III. Accordingly, the absorption spectrum is assumed to be the superposition of a Lorentzian line and a \tan^{-1} edge. The respective widths of the line and the jump were determined to be 5.1 and 3.5 eV. The oscillator strength for the jump was deduced from Cromer's table.¹⁹ The calculated distribution is displayed in Fig. 10. One can verify that the theory provides a fair account of the general behavior of the reflectivity variations in this region. However, at higher values of the glancing angle u it seems again that our model leads to overestimated values of the reflectivity; see below.

V. DISCUSSION

In this paper we have investigated the influence of the anomalous variations of the optical constants on the x-ray reflectivity of mirrors at frequencies close to a characteristic frequency of the material. For this purpose we have carried out transmission and reflection measurements in the spectral ranges corresponding to the M_V photoabsorption regions of three different elements, namely, La, Au, and Th. Our choice was motivated by the fact that these M_V transmission spectra clearly illustrate three different cases of physical interest: The corresponding photoabsorption processes involve final states which are either discrete (La) or belonging to a continuum (Au) or a combination of these two situations (Th).

In order to interpret the spectra of the x-ray radiation specularly reflected under grazing incidence, we have given an analytic expression of the reflectivity R in terms of the optical constants β, δ and of the glancing angle u . This expression, valid for small values of u , enabled us to qualitatively discuss the influence of the variations of β and δ on $R(u)$. Then, the next step was to obtain a reliable estimation of the changes of β and δ in an anomalous region, (i.e., close to a characteristic frequency of an element constituent of the mirror). Since β and δ can be deduced from, respectively, the imaginary and real part of the scattering factor $F(\omega)$, we have derived a simple theoretical method for computing $F(\omega)$ in such anomalous regions. In the absence of any *ab initio* calculation, we have used a semiphenomenological model relying on both experimental data and compiled values for the core-hole widths and the oscillator strengths associated

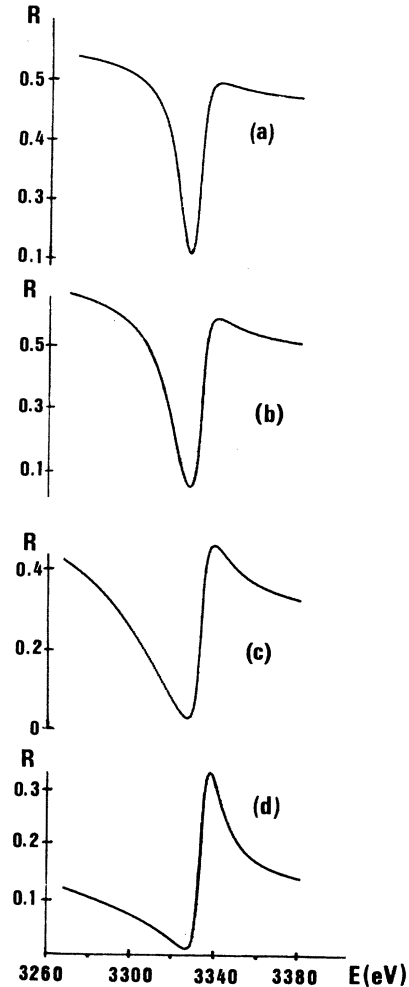


FIG. 10. Reflection spectra for ThF_4 in the M_V -edge-absorption region of Th, at different glancing angles u , obtained from the theoretical model presented in the Sec. III. (a) $u=7$ mrad; (b) $u=9$ mrad; (c) $u=11$ mrad; (d) $u=13$ mrad.

with the transitions considered. A remarkable feature of this model is that it allows us to account for the overall variations of the specular reflectivity in the anomalous regions. It should be noted, however, that precise quantitative comparison between theory and experiment are impeded in fact mainly by the difficulties encountered when trying to obtain reliable absolute measurements of the reflectivity in the x-ray range.⁴ These difficulties can be ascribed to several different causes: One is the very large uncertainty affecting the experimental values of the linear absorption coefficient μ for a given material in the vicinity of an absorption edge. Note that it is an important problem in x-ray spectroscopy and makes clear the need for accurate determinations of μ in various elements, in particular for those studied here which display such typical absorption spectra.

Another source of discrepancy can be the fact that the tables of Cromer and Leroux and Thinh tables, which we have used here, are established for atomic species and may not be convenient for mirrors containing compounds of

these elements, not to mention the effects due to the surrounding atoms in the solid.

Finally another important source of discrepancy may originate from the actual state of the surface of the mirror. As a matter of fact, our simple model assumes the surface is a perfect plane and does not take into account the roughness effects. These effects, which can be important in the x-ray range, generally reduce the reflectivity. This could explain, at least partly, the observed difference between the experiment and the calculation, the latter often leading to overestimated results.

Our poor knowledge of the exact composition of the surface layers of the material contributing effectively to the reflection process can give rise also to a disagreement between theory and experiment. The evaporated coating films (cases of Au and ThF₄ are likely to be inhomogeneous and to present a gradient of electronic density depending on the thickness.²⁸ For glass mirrors (the case of La)

the polishing process often induces modifications of the surface with respect to the bulk. A comprehensive discussion of the influence of these treatments on the reflectivity can be found in Ref 6. Note that the effects of such modifications of the composition of the surface layers can become important for values of $X \simeq 1$ ($u \simeq u_c$). Indeed, for lower values of Y ($Y < 0.63$), small variations of X around $X=1$ can induce substantial modifications in the reflectivity; see Sec. II and Fig. 2(a).

It should be stressed, however, that all these discrepancies are mainly noticeable at relatively large glancing angles and that, on the whole, the agreement between theory and experiment is satisfactory. This fact lends stronger support to our belief that x-ray reflectivity measurements may provide interesting information on the optical constants, the scattering factors and more generally, on inner-shell spectra when other methods are inadequate.⁴ See also Ref. 29.

- ¹V. Rehn and V. O. Jones, *Opt. Eng.* **17**, 504 (1978); M. R. Howells, *Appl. Opt.* **19**, 4027 (1980); D. H. Bilderback and S. Hubbard, *Nucl. Instrum. Meth.* **195**, 91 (1982).
- ²O. A. Ershov, D. A. Goganov, and A. P. Lukirskii, *Fiz. Tverd. Tela (Leningrad)* **1**, 2355 (1965) [*Sov. Phys.—Solid State* **7**, 1903 (1966)].
- ³J. Rife and J. Osantowski, in *Proceedings of the Topical Conference on Reflecting Optics for Synchrotron Radiation*, edited by M. R. Howells (SPIE, Bellingham, 1981).
- ⁴J. M. Andre, A. Maquet, and R. Barchewitz, *Phys. Rev. B* **25**, 5671 (1982).
- ⁵V. Rehn, V. O. Jones, J. M. Elson, and J. M. Bennett, *Nucl. Instrum. Meth.* **172**, 307 (1980) and references therein.
- ⁶L. Nevot and P. Croce, *Rev. Phys. Appl.* **15**, 761 (1980) and references therein.
- ⁷L. A. Smirnov and S. B. Anoklin, *Opt. Spectrosc.* **48**, 315 (1980).
- ⁸M. S. Jensen, *J. Phys. B* **13**, 4337 (1980).
- ⁹T. Fukamachi and S. Hosoya, *Acta Crystallogr. Sect. A* **31**, 215 (1975).
- ¹⁰D. P. Siddons, in *Proceedings of the Topical Conference for Soft X-Ray Diagnostics*, edited by D. T. Attwood and B. L. Menke (AIP, New York, 1981).
- ¹¹M. Hart and D. P. Siddons, *Proc. R. Soc. London, Ser. A* **376**, 465 (1981).
- ¹²C. Bonnelle, R. C. Karnatak, and J. Sugar, *Phys. Rev. A* **9**, 1920 (1974).
- ¹³P. Motais, E. Belin, and C. Bonnelle, *J. Phys. F* **11**, L169 (1981).
- ¹⁴R. Karnatak, J. M. Esteva, and J. P. Connerade, *J. Phys. B* **14**, 4747 (1981).
- ¹⁵C. Mande, *Ann. Phys. (Paris)* **13**, 1559 (1960).
- ¹⁶R. Marmoret, J. M. André, and R. Barchewitz, in *Abstracts of International Conference on X-Ray and Atomic Inner-Shell Physics*, edited by B. Craseman (University of Oregon, Eugene, 1982) (unpublished).
- ¹⁷M. R. Lefevre and M. Montel, *Opt. Acta* **20**, 97 (1973).
- ¹⁸G. Martens and P. Rabe, *J. Phys. C* **14**, 1528 (1981).
- ¹⁹D. T. Cromer, *Acta Crystallogr.* **18**, 17 (1965).
- ²⁰J. Leroux and T. P. Thinh, in *Revised Tables of X-Ray Mass Absorption Coefficients* (Claisse Scientific Corp., Quebec, 1977).
- ²¹*Higher Transcendental Functions, Bateman Manuscript Project*, edited by A. Erdelyi (McGraw-Hill, New York, 1953), Vol. 1.
- ²²R. Barchewitz, Thèse d'Etat, Université Pierre et Marie Curie, Paris, 1977 (unpublished).
- ²³R. Barchewitz, M. Montel, and C. Bonnelle, in *Proceedings of the 5th International Congress on X-Ray Optics and Microanalysis*, edited by G. Möllenstedt and K. H. Gaukler (Springer, Tübingen, 1968).
- ²⁴C. Bonnelle (private communication). Note that the transmission experiment has been performed through a thick (~ 350 Å) screen of La₂O₃, which is likely to lead to an underestimate of the value of μ_{\max} .
- ²⁵Y. Cauchois and C. Sénémaud, *International Tables of Selected Constants, Wavelengths of X-Ray and Absorption Edges* (Pergamon, Oxford, 1978).
- ²⁶R. Barchewitz, M. Cremonese-Visicato, and G. Onori, *J. Phys. C* **41**, 4439 (1978).
- ²⁷G. Lachere, Thèse d'Etat Université Pierre et Marie Curie, Paris, 1979 (unpublished).
- ²⁸L. G. Parratt, *Phys. Rev.* **95**, 359 (1954).
- ²⁹J. Bremer, L. Kaihola, and R. Keski-Kuha, *J. Phys. C* **13**, 2225 (1980).